The Astronomical Journal, 165:256 (12pp), 2023 June https://doi.org/10.3847/1538-3881/acd11b

The True Nature of the Brightest Local Triple Stellar Candidates within 100 pc in the Galaxy

Z. T. Yousef[1], A. Annuar[1], Mashhoor A. Al-Wardat[2,3,4], and N. S. A. Hamid[1]
[1] Department of Applied Physics, Faculty of Science and Technology, Universiti Kebangsaan Malaysia, 43600 UKM Bangi, Selangor, Malaysia; adlyka@ukm.edu.my
[2] Department of Applied Physics and Astronomy, University of Sharjah, P.O. Box 27272 Sharjah, United Arab Emirates
[3] Sharjah Academy for Astronomy, Space Sciences and Technology, University of Sharjah, P.O. Box 27272 Sharjah, United Arab Emirates
[4] Department of Physics, Faculty of Sciences, Al al-Bayt University, P.O. Box: 130040, Mafraq, 25113, Jordan
Received 2022 October 6; revised 2023 April 20; accepted 2023 April 20; published 2023 May 31

Abstract

We present a study of a sample of bright ($V \leqslant 10$ mag) and close ($d \leqslant 100$ pc) triple–stellar system candidates in the galaxy, consisting of eight systems in total. Our aim is to determine their actual multiplicity and the physical properties of each stellar component in the systems. The sample was analyzed using a complex spectrophotometric technique by Al-Wardat that utilizes ATLAS9 line-blanketed plane-parallel model atmospheres. Based on our analysis, we found that five of the systems (HIP 109951, HIP 105947, HIP 40523, HIP 35733, and HIP 23824) are indeed triples, while the remaining three systems (HIP 9642, HIP 59426, and HIP 101227) are more consistent with being quadruples. We estimated the physical properties of the individual components using the most recent parallax measurements from the GAIA Data Release 3 catalog. We also examined the applicability of the well-established Mass–Luminosity (M–L) relation for individual components of all the stellar systems that have been analyzed by the Al-Wardat technique. We found that generally, the components are in good agreement with the established relationship. This further supports the reliability of the method in determining the physical properties of multiple stellar systems. In addition, we investigated the M–L relation for each order of stellar multiplicity (i.e., binary, triple, and quadruple) by performing linear fitting to the data. It was found that the slopes for each multiplicity are consistent with each other. The relations also seem to shift down in luminosity for a given total mass, as the order of multiplicity increases from binary to quadruple.

Unified Astronomy Thesaurus concepts: Multiple stars (1081); Stellar properties (1624); Stellar atmospheres (1584); Stellar evolution (1599)

1. Introduction

The statistics of stellar systems of multiplicity two and higher reveals that they constitute ∼50% of nearby solar-type main-sequence stars (Duquennoy & Mayor 1992). These systems are important as they offer the only direct way to determine stellar masses. This particular parameter can provide crucial clues on the formation and evolution of stars (Ebert 2001). Most identified binary and multiple stellar systems (BMSSs) are classified as close visual BMSSs (CVBMSSs). These systems appear as single stars even with the largest ground-based telescopes due to their very close apparent angular separation (Hilditch 2001). Such systems can only be identified using high-resolution observational techniques, such as speckle interferometry (Labeyrie 1970 and Balega & Tikhonov 1977) and adaptive optics.

The photodynamical modeling technique has been considered as the most common analytical method to determine the nature of BMSSs (i.e., binary, triple, or higher-order systems) and the physical properties of their components. This method combines lightcurve modeling and radial velocity (RV) measurements from catalogs to estimate the stellar properties of binary systems (Borkovits et al. 2016, 2019; Koćak et al. 2020; Sürgit et al. 2020). This approach, however, is only applicable for eclipsing binaries, which represent less than 10% of observed binaries. This makes the photodynamical modeling technique very limited. In 2002, a new spectrophotometric method was developed by Al-Wardat (2002). The method employed speckle interferometry measurements, along with theoretical stellar spectral energy distributions (SEDs), to determine the nature of BMSSs and their stellar properties. The data required to perform this technique can be retrieved from free-access catalogs. It is the only synthetic technique for analyzing all types of BMSSs, including CVBMSSs. This makes it ideal for analyzing BMSSs and finding their physical properties. In fact, a lot of systems have been analyzed using this novel method since 2002 (e.g., Al-Wardat 2002, 2008, 2012; Masda et al. 2016, 2018b, 2019c; Al-Wardat et al. 2021; Yousef et al. 2021; Yousef et al. 2022). These papers used the analysis results to estimate the physical parameters of CVBMSSs, as well as to propose formation and evolution theories for the systems based on the parameters obtained.

In this paper, we present analyses of a sample of bright ($V \leqslant 10$ mag) and the closest ($d \leqslant 100$ pc) triple–stellar system candidates in our galaxy, with sufficient data to perform the Al-Wardat (2002) analysis technique. Our aim is to examine the multiplicity of the systems to verify if they are indeed triple systems, or otherwise, and to estimate the physical properties of each star in the systems. This will allow us to further understand their formation and evolution. This paper is the third paper for this work; the first two papers were case studies on two of the systems in our sample (Yousef et al. 2021 and Yousef et al. 2022).

In Section 2, we describe in more detail our stellar sample. This is followed by the analytical method in Section 3. The results of our analysis are presented in Section 4. In Section 5, we provide a discussion of our results, and finally, in Section 6, we summarize our findings.

2. Sample Selection

Our sample was constructed based on the Catalog of Components of Double and Multiple Stars (CCDM catalog) by Dommanget & Nys (2002). The catalog was first filtered to contain systems that are located within 100 pc from us and have visual magnitudes less than 10 mag. This was then crossmatched with the Multiple Star Catalog (MS catalog) introduced by Tokovinin (2021), to select those that have been identified as triple or higher-order systems based on observations. This means that at least one of the components in each system is a sub-binary. This had motivated us to study the nature of the other component in each system to determine if there was another sub-binary or whether it was merely a single star. Only BMSSs with measured parallax, color indices, and magnitudes were incorporated in our sample, as these parameters are required to perform the analytical method prescribed by Al-Wardat (2002). Given the selection method, the sample is not complete in any sense, nor necessarily representative of the binaries and multiple systems in the solar vicinity. The sample includes eight stellar system candidates in total, namely HIP 9642, HIP 59426, HIP 101227, HIP 109951, HIP 105947, HIP 35733, HIP 40523, and HIP 23824. Systems HIP 101227, HIP 10995, and HIP 105947are classified as CVBMSs. The parallaxes of the systems were retrieved from the GAIA Data Release 3 (DR3) catalog. Mardini et al. (2022) presented corrections for the parallaxes observed by GAIA DR3. Anyway, all of the systems in our sample are not affected by these corrections. The analyses for HIP 101227 and HIP 23824 were published in Yousef et al. (2021) and Yousef et al. (2022). Therefore, they will only be included in the discussion and conclusion of this paper. Sections 2.1–2.6 present the basic descriptions of the six remaining systems analyzed in this study, sorted according to their distances.

2.1. HIP 59426

The triple-system candidate HIP 59426 is located at an R.A. of $12^{h}11^{m}22^{s}91$ and a decl. of $-16°47'27''03$ (SIMBAD catalog). The system's distance obtained from the GAIA catalog is 34.07 ± 0.027 pc. Based on the CCDM catalog, this is a binary system with two stars, A and B. However, Nordström et al. (2004) observed double lines in the spectrum of the star A, indicating that it is a sub-binary system with components Aa and Ab. Meanwhile, Tokovinin (2019) reported that the period of the sub-binary system was $P = 212$ days, with a mass ratio of 0.874 between components Aa and Ab.

2.2. HIP 9642

The HIP 9642 system is located at a distance of 50.03 ± 0.05 pc, based on the GAIA catalog. The system is at an R.A. of $02^{h}03^{m}55^{s}25$ and a decl. of $-45°24'46''.46$ (SIMBAD catalog). The system is a binary system with two stars, A and B, according to the CCDM catalog. On the other hand, Nordström et al. (2004) claimed it as a sub-binary system upon detecting a double-lined RV spectrum for component A, which suggested that star A is not a single star. The study estimated a mass ratio of 0.86 between components Aa and Ab. Tokovinin (2016) revised the orbit of HIP 9642 in accordance with the most recent data and presented new dynamical parameters for the main orbit as follows: $P = 415.0$ days, $a = 1.659$ mas, $e = 0.2645$, and $i = 36.^{\circ}0$. The study also built an orbit for the sub-binary system A with the following parameters: $P = 4.78$ days, $a = 0.1002$ mas, and $e = 0$.

2.3. HIP 109951

HIP 109951 is a close visual stellar system located at an R.A. of $22^{h}16^{m}06^{s}56$ and a decl. of $-07°05'26''62$ (SIMBAD catalog). The revised distance of this system from the earth obtained from the GAIA catalog is 56.82 ± 0.98 pc. Referring to the CCDM catalog, HIP 109951 is a binary system with two components, A and B. On the other hand, Nordström et al. (2004) noted a single-line RV for component B, indicating that this component is not a single star. The first orbit for HIP 109951 was built by Horch et al. (2009) using the orbital analyzing method proposed by MacKnight & Horch (2004). The adopted orbital parameters result in a mass sum $M_{\rm tot} = 2.98 \pm 0.91 M_{\odot}$, using the old Hipparcos parallax of 15.04 ± 1.52 mas (SIMBAD catalog). A study by Masda et al. (2019a) estimated the physical parameters of the system as a triple, based on the revised Hipparcos parallax of Van Leeuwen (2007), using the method initiated by Al-Wardat (2002). Masda et al. (2019a) modified the orbit of the system by using the Docobo method and estimated a total dynamical mass of $2.59 \pm 0.4 M_{\odot}$ and $2.15 \pm 0.35 M_{\odot}$, based on the old parallax from GAIA DR2 and the revised Hipparcos parallax, respectively. Meanwhile, the total mass of the system obtained using the Al-Wardat (2002) method is $M_{\rm tot} = 2.55 \pm 0.38 M_{\odot}$. Turning to this present study, the system was analyzed using the revised parallax from the GAIA catalog.

2.4. HIP 35733

The HIP 35733 system is located at an R.A. of $07^{h}22^{m}16^{s}37$ and a decl. of $-35°54'58''46$ (SIMBAD catalog). The system is 58.69 ± 0.6 pc from the earth based on the GAIA catalog. The CCDM catalog shows that HIP 35733 is a binary system with two components, A and B. The double-lined RV in star A was observed by Nordström et al. (2004), signifying that the component is not a single star. Tokovinin (2019) indicated that the main binary of HIP 35733 is a wide physical binary system with a period of $P = 5$ Kyr. The study also estimated the individual masses of the triple-system components as follows: $M_{Aa} = 1.22 \pm 0.20 M_{\odot}$, $M_{Ab} = 1.19 \pm 0.20 M_{\odot}$, and $M_{B} = 1.16 \pm 0.20 M_{\odot}$.

2.5. HIP 105947

HIP 105947 is a close visual system located at a distance of 64.56 ± 0.053 pc from the earth based on the GAIA catalog. The system is at an R.A. of $02^{h}03^{m}55^{s}.25$ and a decl. of $-45°24'46''46$ (SIMBAD catalog). Referring to the CCDM catalog, HIP 105947 is a binary system with two components, A and B. Nordström et al. (2004) observed a double-lined RV spectrum for component A, affirming that the star is a sub-binary system. The system was also determined as binary by Balega et al. (2006), Mason et al. (2010), and Masda et al. (2018b). The first orbit for HIP 105947 was built by Balega et al. (2006), using the Monet (1979) orbital analysis method. The adopted orbital parameters disclosed a mass sum of

$2.68 \pm 0.01 M_{\odot}$. Mason et al. (2010) modified the orbit of the system using the newly released positional measurements and estimated a mass sum of $2.30 \pm 1.14 M_{\odot}$. The most recent analyses for HIP 105947 were performed by Masda et al. (2018b) and Tokovinin (2019). Masda et al. (2018b) estimated the physical parameters of the system as a binary using the Al-Wardat (2002) method. The study revised the orbit of the system based on the most up to date positional measurements using the method initiated by Tokovinin (1992), the updated orbital parameter by Masda et al. (2018b), and the revised parallax from the GAIA catalog, which resulted in the estimated mass sum for the system as $2.95 \pm 0.36 M_{\odot}$.

Tokovinin (2019) analyzed the system as triple in A. The study estimated the individual masses of the system by depending on the orbital analysis and by using the revised parallax from the Hipparcos catalog compiled by Van Leeuwen (2007). The individual masses are as follows: $M_{Aa} = 1.25 M_{\odot}$, $M_{Ab} > 0.35 M_{\odot}$, and $M_B = 0.96 M_{\odot}$. In his study, Tokovinin (2019) also estimated the individual masses of the main binary system using the RV amplitudes and the inclination of the outer orbit, which is parallax-independent. These are as follows: $M_A = 1.61 M_{\odot}$, $M_B = 0.62 M_{\odot}$.

2.6. HIP 40523

The system HIP 40523 is located at an R.A. of $08^{h}16^{m}26^{s}.47$ and a decl. of $-03°13'33''92$ (SIMBAD catalog). The distance of the system obtained from the GAIA catalog is 77.87 ± 0.14 pc. The CCDM catalog suggests that HIP 40523 is a binary system. Nordström et al. (2004) claimed that the system is a sub-binary system by detecting a double-lined RV spectrum for component A, which suggested that the star A is not a single star. star. Tokovinin (2019) presented the dynamical parameters of the sub-binary orbit as follows: $P = 28.96$ days, $e = 5.24$, and $i = 62.^{\circ}0$. The study also estimated a mass ratio of 0.998 between the components of the sub-binary A.

The location information and prior studies of HIP 101227 and HIP 23824 can be found in Yousef et al. (2021) and Yousef et al. (2022), respectively.

3. Methodology

In this work, we analyzed our sample using the spectrophotometric technique proposed by Al-Wardat (2002). Based on this method, several atmosphere models were developed for the systems. These models were tested in a process called synthetic photometry, to select the best-fitting model that belongs to the most likely nature of the system and to determine its physical parameters. Further details about the methodology used are discussed in Sections 3.1 and 3.1.1.

Each system was first analyzed assuming that it is a triple system. Then, the results were used to position the stellar components on the isochrone and evolutionary tracks for low- and intermediate-mass stars with different metallicities derived by Girardi et al. (2000). This was performed to determine if their metallicities, ages, and masses are consistent with them being triple systems. If the results are consistent with the system being a triple, we stopped our analysis here. If the results indicated otherwise, we continued our analysis to higher-order multiplicity, until we obtained reliable results (Al-Wardat 2002).

3.1. Atmospheric Modeling

The Al-Wardat (2002) method is a spectrophotometric technique that employs Kurucz's (ATLAS9) blanketed model grids to construct the synthetic SEDs of the individual components of the stellar system analyzed. Special software in FORTRAN was used to combine the individual SEDs to obtain the entire synthetic SED model for the system. The atmospheric modeling involves several stages. First, we build the SEDs for the main binary components, A and B. Then, we build the SEDs for the triple-system components (i.e., the components of the sub-binary star A and the single star B and vice versa). Next, we build the SEDs for the quadruple system (i.e., the components of the sub-binaries A and B). SEDs for higher-order multiplicities were built if a good fit could not be obtained for any of the previous multiplicities.

In order to build the SED models for the components, the average value of the magnitude differences (Δm) between the main components of the system in the visual band must be determined. This was calculated from Δm measurements corresponding to V-band filters in the fourth catalog (The Fourth Catalog of Interferometric Measurements of Binary Stars). Then, the average value for Δm and the entire visual magnitude (m_v) were used in the following equations to estimate the apparent magnitudes for the individual components A and B:

$$m_V^A = m_v + 2.5 \log (1 + 10^{-0.4 \Delta m}), \quad (1)$$

$$m_v^B = m_v^A + \Delta m, \quad (2)$$

$$M_v = m_v + 5 - 5 \log d - A_v. \quad (3)$$

Next, the effective temperature ($T_{\rm eff}$), mass, spectral type ($S_{\rm p}$), and bolometric correction (BC) obtained from Gray (2005) and Lang (1992), along with the individual apparent magnitudes (m_v^A and m_v^B), were used to compute the luminosity (L), radius (R), and the surface gravity ($\log g$) of the stars using the following well-known equations:

$$M_{\rm bol} = M_{\rm bol}^{\odot} - 2.5 \log (L/L_{\odot}), \quad (4)$$

$$\log (R/R_{\odot}) = 0.5 \log (L/L_{\odot}) - 2 \log (T_{\rm eff}/T_{\rm eff_{\odot}}), \quad (5)$$

$$\log g = \log (M/M_{\odot}) - 2 \log (R/R_{\odot}) + 4.43. \quad (6)$$

The estimated values obtained for $T_{\rm eff}$, R, and $\log g$ were used as the initial input parameters for the grids of Kurucz's plane-parallel models (ATLAS9) to obtain preliminary synthetic SEDs for the main stars A and B. Then the main star's SEDs were combined to obtain the entire synthetic SED of the system using the Al-Wardat (2002) technique. This technique combines the individual SEDs according to the following equation (Al-Wardat 2012):

$$F_{\lambda} \cdot d^2 = H_{\lambda}^A \cdot R_A^2 + H_{\lambda}^B \cdot R_B^2, \quad (7)$$

expressed as:

$$F_{\lambda} = (R_A/d)^2 (H_{\lambda}^A + H_{\lambda}^B (R_A/R_B)^2), \quad (8)$$

where F_{λ} is the SED of the entire system. H_{λ}^A and H_{λ}^B represent the flux from the unit surface of the binary components A and B, respectively. In the case of more than two components in the system, we used the following equation (Al-Wardat 2002;

Al-Wardat et al. 2021):

$$F_\lambda \cdot d^2 = \sum_{i=1}^{N} H_\lambda^i \cdot R_i^2, \quad (9)$$

where F_λ is the flux for the entire component of the multiple system, d is the distance to the system in parsecs, N is the number of components, and R_i are the radii of the component in solar units $R_\odot$. H_λ^i are the fluxes of the component in units of ergs $cm^{-2}s^{-1}$ $Å^{-1}$.

To select the best-fitted SED model with the most accurate physical properties for the system, atmosphere modeling was performed in an iterative manner with initial input parameters for ATLAS9. This was executed until the synthetic magnitudes and color indices obtained were in agreement with those obtained from observations (SIMBAD catalog).

To test the reliability of the results obtained, the best-fitted SED model adopted from the atmospheric modeling was then compared with observational SEDs from past studies, if available. Both the observed and synthetic SEDs should have similar profiles and shapes of continuum. Synthetic magnitudes and color indices can be calculated from the synthetic SED using the following equation (Al-Wardat 2002, 2008, 2012):

$$m_p = -2.5 \log \frac{\int P_p(\lambda) F_{\lambda,s}(\lambda) d\lambda}{\int P_p(\lambda) F_{\lambda,r}(\lambda) d\lambda} + ZP_p, \quad (10)$$

where m_p represents the synthetic magnitude of the passband p, P_p is the dimensionless sensitivity function of the passband p, and $F_{\lambda,s}(\lambda)$ and $F_{\lambda,r}(\lambda)$ are the synthetic SEDs of the star being studied and the reference star (Vega in this case), respectively. The zero-points, ZPp, were retrieved from Apellániz (2007).

3.1.1. Physical Properties of the System

After determining the best-fitted SED, the physical properties of the individual components of the systems can then be determined. Some properties were obtained directly from the adopted best-fitted SED results, namely: $T_{\rm eff}$, R, and $\log g$. On the other hand, the luminosity of the individual components of the systems needs to be calculated using the formula for stellar luminosity derived directly from the well-known Stefan–Boltzmann law (Halliday et al. 2013).

Meanwhile, to calculate the apparent magnitude for the components, the absolute magnitude must first be determined. Both the absolute magnitude $M_{(\rm abs.)}$ and luminosity L are related, based on the following formula:

$$M_{(\rm abs.)} = -2.5 \log(L/L_o), \quad (11)$$

where L_o is the zero-point luminosity, which equals 3.01310^{28} W (Mamajek et al. 2015). Next, the following apparent magnitude formula was applied to calculate the apparent magnitude of the stars for the component:

$$M_{\rm app} = M_{(\rm abs)} - 5 + 5 \log(d). \quad (12)$$

The masses of the individual components were estimated based on the positions of the components on the evolutionary track diagram derived by Girardi et al. (2000), while the spectral types of the components were determined based on their temperatures. The ages of the systems, on the other hand, were estimated based on their positions on the isochrone tracks for low- and intermediate-mass stars with different metallicities (Girardi et al. 2000), as follows:

$$t_{\rm ms} = f_{\rm ASITR}(m_{A,B} - 5 \log d + 5 - A, Z), \quad (13)$$

where $f_{\rm ASITR}$ is the age of the synthetic isochrones track function and Z is the component metallicity. If none of the components of the system are moving away from the main sequence, then there are numerous isochrones that can pass through all the components of the system on the HR diagram. Hence, only if at least one of the system's components has already evolved out of the main sequence does this equation have a singular solution (within the error values of the observations), which is the case for all of the stars in this sample, as shown in Figure 2.

Table 1
A Comparison between the Adopted Physical Parameters for HIP 109951 in This Work and from Masda et al. (2019a)

Physical Parameter	Component	This Work	Masda et al. (2019a)
$T_{\rm eff}(K)$	A	5850 ± 80	5836 ± 80
	B_a	4900 ± 80	5115 ± 80
	B_b	4100 ± 80	4500 ± 80
$R(R_\odot)$	A	4.72 ± 0.28	1.09 ± 0.04
	B_a	0.69 ± 0.02	0.60 ± 0.05
	B_b	0.41 ± 0.02	0.49 ± 0.06
$\log g$	A	4.45 ± 0.06	4.45 ± 0.06
	B_a	4.60 ± 0.07	4.60 ± 0.06
	B_b	4.65 ± 0.07	4.65 ± 0.06

4. Analysis and Results

In this section, we present the analysis results for each of the stellar systems in our sample (Sections 4.1–4.6), except for HIP 101227 and HIP 23824, as their results have been published previously (Yousef et al. 2021; Yousef et al. 2022). All synthetic photometries measured are tabulated in Table 2. The SEDs, evolutionary tracks, and isochrone tracks are presented in Figures 1 and 2, respectively. Table 4 lists the final physical parameters determined for all systems.

4.1. HIP 59426

Nordström et al. (2004) reported double lines in the spectrum of component A of the HIP 59426 system. This confirmed that component A is a sub-binary system. Hence, HIP 59426 at least consists of three components, which are Aa, Ab, and B. The other case is that the system HIP 59426 is quadruple, i.e., it consists of the components Aa, Ab, Ba, and Bb. In order to decide which case of multiplicity is more likely for the system, the analysis was first performed by assuming that the system is triple in A.

Next, the physical properties obtained after analyzing HIP 59426 as triple in A were applied to position them on both evolutionary and isochrone tracks. Notably, the position of the B component was located outside the isochrone tracks. This negates the possibility that HIP 59426 is a triple system.

The analysis was then continued by assuming that the system is quadruple (has four components). These are Aa and Ab, belonging to the sub-binary A, and Ba and Bb, belonging to the sub-binary B. The analysis denotes good fitting results for both sub-binary systems. Table 2 presents the final results of the synthetic magnitudes and color indices within three photometrical systems (Johnson-Cousins, Stromgren, and Tycho) of

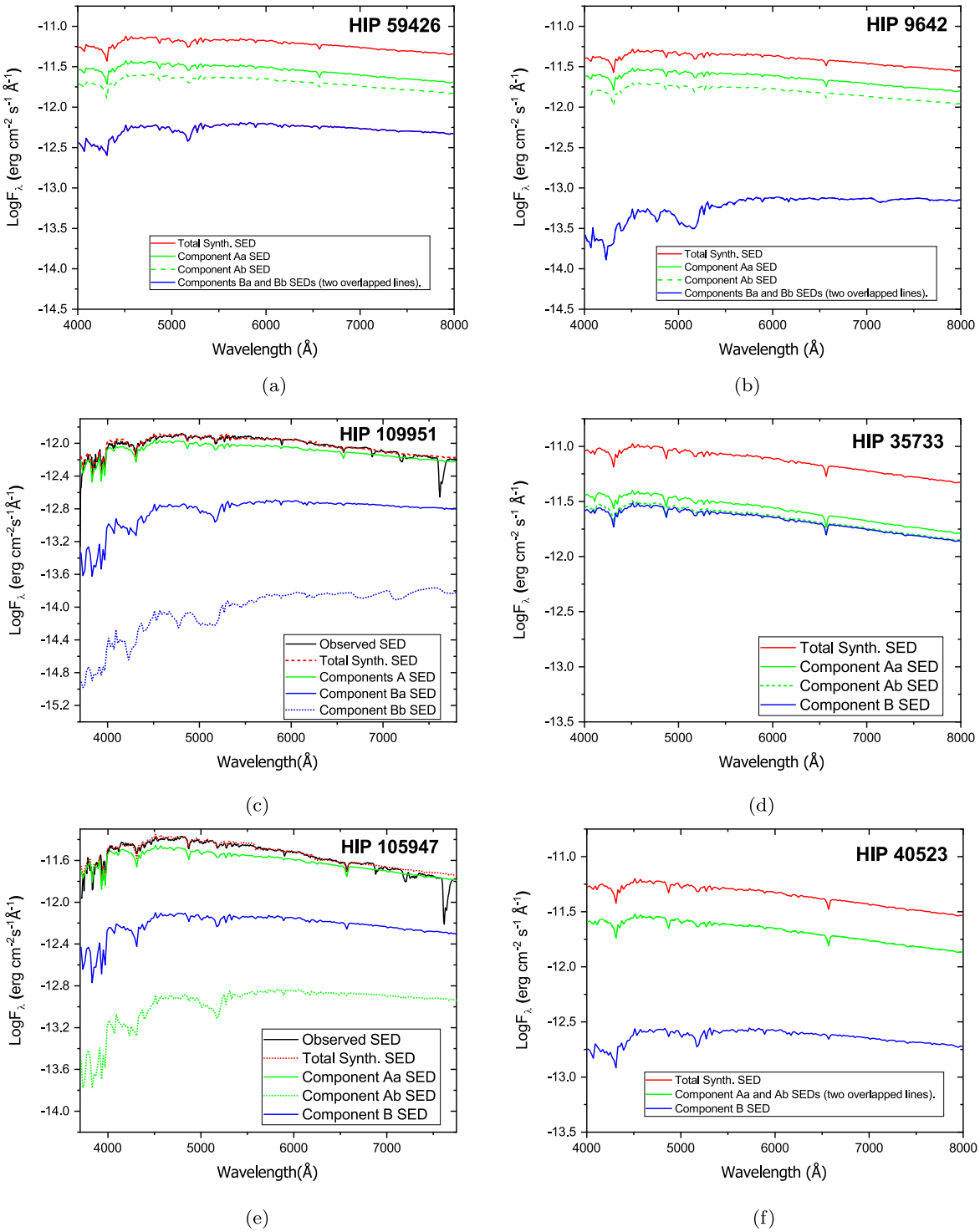

Figure 1. The best-fit synthetic SEDs for the individual components and entire systems studied in this work.

the entire system. The consistency of the results is displayed by comparing synthetic and observed photometry (see Table 3). The adopted synthetic SED is shown in Figure 1(a). The RUWE parameter is known to be a good indicator of (unresolved) binaries in the GAIA astrometric fits, as values slightly greater than 1.0 may indicate possible multiplicity (Stassun & Torres 2021); for HIP 59426, the values of RUWE for the components *A* and *B* are 10.73 and 1.1, respectively. These advocate that both components have an extra sub-component, supporting HIP 59426 quadruplicity.

Referring to the adopted physical properties of the quadruple system (see Table 4), the components of the system were positioned on the stellar evolutionary tracks and stellar isochrone tracks. These are illustrated in Figure 2(a). The positions of the components on the evolutionary tracks (see Figure 2(a)) depict the following individual masses: $M_{Aa} = 0.99 \pm 0.20 M_{\odot}$, $M_{Ab} = 0.95 \pm 0.20 M_{\odot}$, $M_{Ba} = 0.80 \pm 0.20 M_{\odot}$, and $M_{Bb} = 0.80 \pm 0.20 M_{\odot}$. Based on the positions of the components on the isochrones diagram (see Figure 1) and using Equation (13), the age of the system was estimated to

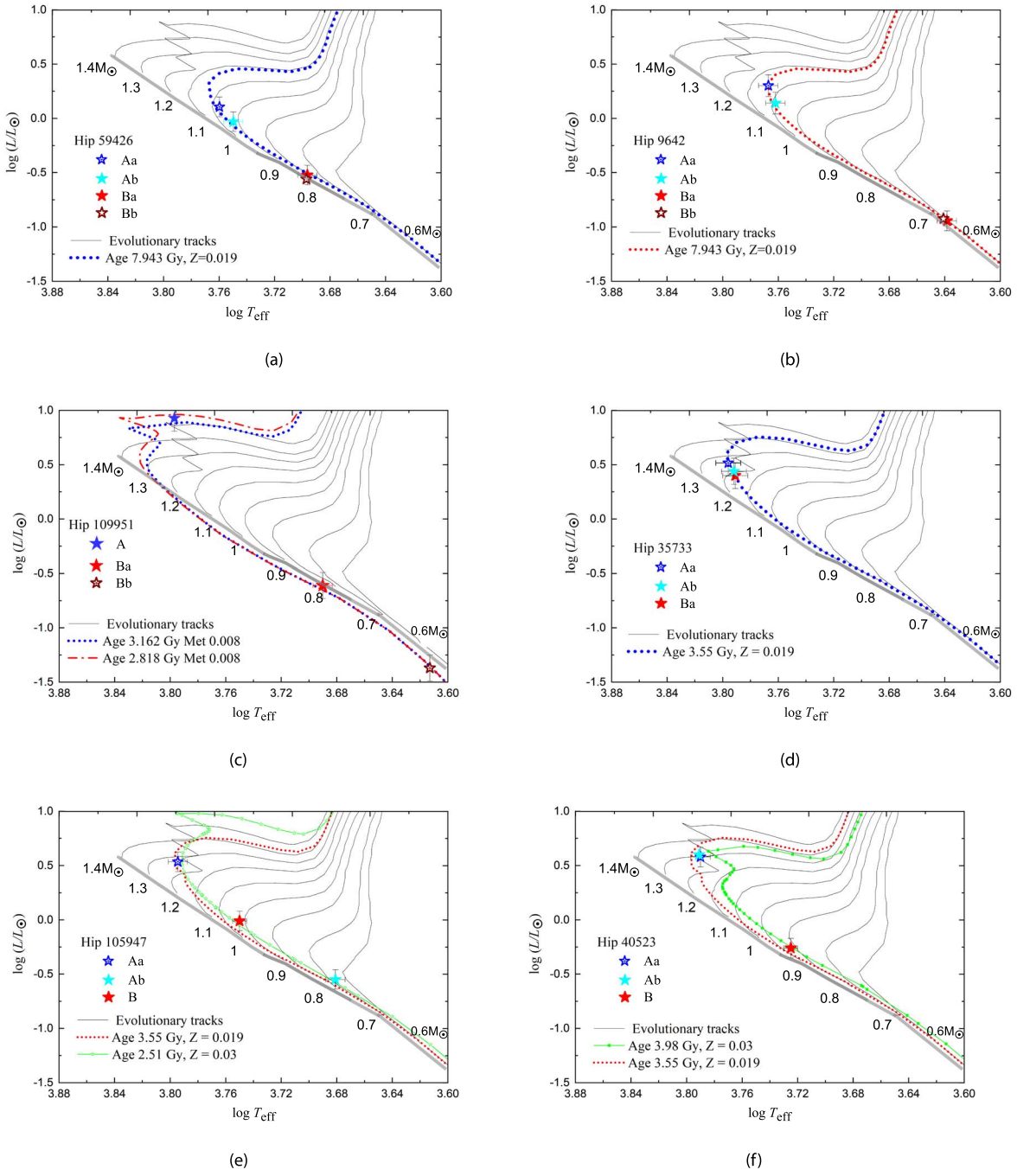

Figure 2. The positions of the individual components for each stellar system on the evolutionary and isochrone tracks for low- and intermediate-mass stars.

be 7.948 ± 0.005 Gyr. The figure also shows that the metallicity of the system components is 0.019.

4.2. HIP 9642

The component *A* of the system HIP 9642 has been confirmed as a sub-binary by Nordström et al. (2004), as they found a double-lined RV in the component spectrum. Thus, the analysis for HIP 9642 was started as triple in *A*. In case we do not get good fitting results for the system as triple in *A*, we check the multiplicity of the component *B* (if it is another binary, as component *A*), by assuming that the system HIP 9642 is a quadruple system.

Depending on the adopted physical properties of HIP 9642 as a triple system in *A*, the components were positioned on both stellar evolutionary and stellar isochrone tracks. However, the position of component *B* was located outside the isochrone tracks. Hence, HIP 9642 is not consistent with the triplet case. Next, the system was assessed as a quadruple (four components). These refer to the components of sub-binary systems *A* and *B*. The analysis gave good fitting results for both sub-binary systems. The synthetic photometry results are presented in Table 2. The consistency of our results is displayed by comparing synthetic and observed photometry (see Table 3). The adopted synthetic SED is shown in Figure 1(b). The RUWE values for the HIP 9642 components are 1.24 and 2.56 for *A* and *B*, respectively. These values

Table 2
The Magnitudes and Color Indices of the Entire Synthetic SED

System	FILTER	HIP 59426	HIP 9642	HIP 109951	HIP 35733	HIP 105947	HIP 40523
Johnson-Cousins	U	7.94 ± 0.04	8.22 ± 0.04	9.66 ± 0.04	7.24 ± 0.04	8.24 ± 0.04	7.84 ± 0.04
	B	7.63 ± 0.04	8.00 ± 0.04	9.42 ± 0.04	7.17 ± 0.04	8.13 ± 0.04	7.75 ± 0.04
	V	6.87 ± 0.04	7.31 ± 0.04	8.70 ± 0.04	6.62 ± 0.04	7.53 ± 0.04	7.16 ± 0.04
	R	6.45 ± 0.04	6.93 ± 0.03	8.30 ± 0.04	6.31 ± 0.03	7.20 ± 0.04	6.84 ± 0.04
	U–B	0.31 ± 0.01	0.21 ± 0.01	0.24 ± 0.03	0.06 ± 0.02	0.12 ± 0.04	0.10 ± 0.02
	B–V	0.76 ± 0.02	0.69 ± 0.02	0.72 ± 0.02	0.56 ± 0.02	0.60 ± 0.02	0.58 ± 0.02
	V–R	0.42 ± 0.03	0.38 ± 0.02	0.30 ± 0.01	0.31 ± 0.02	0.33 ± 0.03	0.32 ± 0.01
Stromgren	u	9.09 ± 0.04	9.37 ± 0.04	10.81 ± 0.04	8.40 ± 0.04	9.41 ± 0.04	9.00 ± 0.04
	v	8.04 ± 0.04	8.37 ± 0.04	9.80 ± 0.04	7.48 ± 0.04	8.46 ± 0.04	8.75 ± 0.04
	b	7.29 ± 0.04	7.70 ± 0.04	9.10 ± 0.04	6.93 ± 0.04	7.87 ± 0.04	8.07 ± 0.04
	y	6.83 ± 0.04	7.28 ± 0.00	8.67 ± 0.04	6.59 ± 0.04	7.50 ± 0.04	7.49 ± 0.04
	u–v	1.05 ± 0.04	0.99 ± 0.04	1.01 ± 0.04	0.91 ± 0.04	0.95 ± 0.04	0.94 ± 0.04
	u–b	0.75 ± 0.02	0.68 ± 0.01	0.71 ± 0.04	0.55 ± 0.01	0.59 ± 0.03	0.57 ± 0.03
	b–y	0.46 ± 0.01	0.42 ± 0.02	0.43 ± 0.01	0.34 ± 0.01	0.37 ± 0.02	0.36 ± 0.01
Tycho	B_T	7.81 ± 0.04	8.18 ± 0.04	9.60 ± 0.04	7.30 ± 0.04	8.27 ± 0.04	7.89 ± 0.04
	V_T	6.95 ± 0.04	7.41 ± 0.04	8.78 ± 0.04	6.68 ± 0.04	7.59 ± 0.04	7.23 ± 0.04
	$B_T - V_T$	0.88 ± 0.02	0.77 ± 0.02	0.82 ± 0.02	0.63 ± 0.02	0.68 ± 0.02	0.66 ± 0.02

support the existence of an extra subcomponent for both *A* and *B*. Therefore, the RUWE values in GAIA DR3 support our results for this system. Next, the components of the system were positioned on both stellar evolutionary and stellar isochrone tracks, based on the adopted physical properties of the quadruple system (see Table 4). Based on Figure 2(b), the locations of the components on the evolutionary tracks gave individual masses as follows: $M_{Aa} = 1.05 \pm 0.20 M_{\odot}$, $M_{Ab} = 0.99 \pm 0.20 M_{\odot}$, $M_{Ba} = 0.60 \pm 0.20 M_{\odot}$, and $M_{Bb} = 0.60 \pm 0.20 M_{\odot}$. Based on the positions of the components on the isochrones diagram (Figure 2), and Equation (13), we determined that the age of the system is 7.943 ± 0.005 Gyr, with a metallicity of 0.19.

4.3. HIP 109951

The stellar system HIP 109951 was previously analyzed utilizing the Al-Wardat (2002) method by Masda et al. (2019a). Turning to this present study, the system was analyzed using the revised data. These are the parallax from the GAIA DR3 catalog and the magnitude difference for the sub-binary system from the MS catalog (Tokovinin 2021). This is done by assuming HIP 109951 as a triple in *B*, as confirmed by Nordström et al. (2004) and Masda et al. (2019a). The present study has slightly modified the effective temperature and the radius compared with those obtained by Masda et al. (2019a). The estimated values of log *g* for all components were not affected by the revised data. This is shown through the comparison in Table 1.

Table 2 shows the final results of the synthetic magnitudes and color indices based on three photometrical systems (Johnson-Cousins, Stromgren, and Tycho) of the entire system. The analysis gave good fitting results for both main and sub-binary. This is displayed by comparing the synthetic and observed photometry (see Table 3). This finding is supported by the observed SED from Al-Wardat (2002), which matches well with our synthetic SED (see Figure 1(c)).

Based on the adopted physical parameters of the triple system (Table 4), the system components were placed on stellar evolutionary and stellar isochrone tracks (see Figure 2(c)). The positions of the components on the evolutionary tracks gave the following individual masses: $M_A = 1.10 \pm 0.20 M_{\odot}$,

Table 3
Comparison between the Total Magnitudes Determined from the Best-fit Synthetic SED and Those Obtained from Observations (SIMBAD Catalog)

HIP	System	Filter	SIMBAD Database (mag.)	This Work (mag.)
59426	Johnson-Cousins	*V*	6.88 ± 0.03	6.87 ± 0.04
		B–V	0.77 ± 0.01	0.76 ± 0.02
	Tycho	B_T	7.77 ± 0.01	7.81 ± 0.04
		V_T	6.91 ± 0.01	6.95 ± 0.04
		Δm	⋯	1.70 ± 0.02	1.70 ± 0.03
9642	Johnson-Cousins	*V*	7.30 ± 0.04	7.31 ± 0.04
		B–V	0.69 ± 0.01	0.69 ± 0.02
	Tycho	B_T	8.15 ± 0.01	8.18 ± 0.04
		V_T	7.40 ± 0.01	7.41 ± 0.04
		Δm	⋯	3.89 ± 0.05	3.89 ± 0.04
109951	Johnson-Cousins	*V*	8.72 ± 0.04	8.70 ± 0.04
		B–V	0.71 ± 0.01	0.72 ± 0.02
	Tycho	B_T	9.58 ± 0.03	9.59 ± 0.04
		V_T	8.81 ± 0.02	8.78 ± 0.04
		Δm	⋯	1.88 ± 0.05	1.88 ± 0.04
35733	Johnson-Cousins	*V*	6.68 ± 0.03	6.62 ± 0.04
		B–V	0.56 ± 0.01	0.56 ± 0.02
	Tycho	B_T	7.28 ± 0.01	7.30 ± 0.04
		V_T	6.69 ± 0.01	6.68 ± 0.04
		Δm	⋯	0.96 ± 0.02	0.98 ± 0.04
105947	Johnson-Cousins	*V*	7.53 ± 0.04	7.55 ± 0.04
		B–V	0.60 ± 0.02	0.60 ± 0.02
	Tycho	B_T	8.24 ± 0.01	8.27 ± 0.04
		V_T	7.59 ± 0.01	7.59 ± 0.04
		Δm	⋯	1.53 ± 0.03	1.53 ± 0.04
40523	Johnson-Cousins	*V*	7.16 ± 0.04	7.16 ± 0.04
		B–V	0.58 ± 0.01	0.58 ± 0.02
	Tycho	B_T	7.93 ± 0.01	7.89 ± 0.04
		V_T	7.30 ± 0.01	7.23 ± 0.04
		Δm	⋯	3.19 ± 0.05	3.19 ± 0.04

Table 4
The Adopted Physical Parameters of Each Component in the Stellar Systems Studied

System	Components	Mass ($M_\odot$)	Luminosity ($L_\odot$)	$T_{\rm eff}$ (K)	R ($R_\odot$)	log g
HIP 59426	*Aa*	0.99	1.27	5750 ± 30	1.14 ± 0.02	4.40 ± 0.05
	Ab	0.95	0.93	5620 ± 30	1.02 ± 0.02	4.40 ± 0.05
	Ba	0.80	0.30	4970 ± 20	0.74 ± 0.01	4.50 ± 0.05
	Bb	0.80	0.30	4970 ± 20	0.74 ± 0.01	4.50 ± 0.05
HIP 9642	*Aa*	1.05	2.0	5850 ± 50	1.38 ± 0.02	4.40 ± 0.05
	Ab	0.99	1.39	5730 ± 30	1.20 ± 0.02	4.40 ± 0.05
	Ba	0.60	0.11	4350 ± 20	0.59 ± 0.05	4.50 ± 0.05
	Bb	0.60	0.11	4350 ± 20	0.59 ± 0.05	4.50 ± 0.05
HIP 109951	*A*	1.10	1.05	5850 ± 80	1.09 ± 0.02	4.45 ± 0.06
	Ba	0.82	0.25	4900 ± 80	0.69 ± 0.02	4.60 ± 0.07
	Bb	0.60	0.04	4100 ± 80	0.41 ± 0.02	4.65 ± 0.07
HIP 35733	*Aa*	1.24	3.06	6430 ± 30	1.41 ± 0.02	4.30 ± 0.05
	Ab	1.24	2.59	6260 ± 30	1.37 ± 0.02	4.30 ± 0.05
	B	1.10	2.45	5900 ± 20	1.50 ± 0.01	4.40 ± 0.05
HIP 105947	*Aa*	1.28	3.42	6230 ± 30	1.59 ± 0.02	4.30 ± 0.05
	Ab	0.88	0.25	4800 ± 30	0.72 ± 0.02	4.50 ± 0.05
	B	0.70	0.99	5500 ± 20	1.10 ± 0.01	4.45 ± 0.05
HIP 40523	*Aa*	1.20	4.35	6170 ± 30	1.83 ± 0.02	4.30 ± 0.05
	Ab	1.20	4.35	6170 ± 30	1.83 ± 0.02	4.30 ± 0.05
	B	0.89	0.58	5200 ± 20	0.94 ± 0.01	4.50 ± 0.05

$M_{Ba} = 0.82 \pm 0.20 M_\odot$, and $M_{Bb} = 0.60 \pm 0.20 M_\odot$. This resulted in a total mass of $M_{\rm tot} = 2.52 \pm 0.35 M_\odot$. These values are consistent with those estimated in prior studies. Besides, Figure 2(c) depicts a metallicity of $Z = 0.008$ for all HIP 109951 components, which equals the metallicity given by Aguilera-Gómez et al. (2018). Based on the positions of the components on the isochrone tracks diagram (see Figure 2(c)), and referring to Equation (13), the age of the system is estimated to be 2.818 ± 0.005 Gyr.

4.4. HIP 35733

The HIP 35733 system was first analyzed by assuming it as triple in *A*, since component *A* is confirmed as sub-binary by Nordström et al. (2004). The analysis of the system as triple in *A* gave good fitting results for both the main and sub-binary systems. Table 2 presents the final results of the calculated magnitudes and color indices based on three photometrical systems (Johnson-Cousins, Stromgren, and Tycho) of the entire system. The apparent magnitudes of the adopted synthetic photometry are similar to those from the observed photometry. This is shown by comparing synthetic and observed photometry (see Table 3). This confirms the consistency of the results reported in the present study. The adopted synthetic SED is shown in Figure 1(d).

Based on the adopted physical parameters of the system as triple in *A* (Table 4), the components of the system were positioned on stellar evolutionary and stellar isochrone tracks (see Figure 2(d)). The positions of the components on the evolutionary tracks revealed the following individual masses: $M_{A_a} = 1.29 \pm 0.40 M_\odot$, $M_{A_b} = 1.20 \pm 0.40 M_\odot$, and $M_B = 1.20 \pm 0.40 M_\odot$. The mass values for the components *Ab* and *B* are consistent with those estimated by Tokovinin (2019; $M_{Aa} = 1.22 M_\odot$, $M_{Ab} = 1.19 M_\odot$, and $M_B = 1.16 M_\odot$). Figure 2(d) shows a metallicity of $Z = 0.019$ for all HIP 35733 components. Based on the positions of the components on the isochrone tracks diagram (Figure 2(d)), and referring to Equation (13), the age of the system is 3.55 ± 0.05 Gyr.

4.5. HIP 105947

Component *A* of HIP 105947 is confirmed as a sub-binary system by Nordström et al. (2004). Hence, the analysis for the system in this study began by assuming that it is a triple system. The analysis gave good fitting results for both the main and sub-binary systems. The entire synthetic photometry results are tabulated in Table 2. The consistency of our results is displayed in the synthetic photometry results (see Table 3). This is also supported by the observed SED reported by Al-Wardat (2002) and the synthetic SED recorded in this present study (Figure 1(e)).

Based on the adopted physical parameters of the triple in *A* given in Table 4, the components of the system were positioned on the stellar evolutionary and stellar isochrone tracks (see Figure 2(e)). The positions of the components on the evolutionary tracks gave the following individual masses: $M_{Aa} = 1.28 \pm 0.20 M_\odot$, $M_{Ab} = 0.99 \pm 0.20 M_\odot$, and $M_B = 0.70 \pm 0.20 M_\odot$. The values appear compatible with the masses estimated in past studies. Based on the positions of the components on the isochrone tracks diagram (see Figure 2(e)), and referring to Equation (13), the age of the system lies between 2.51 ± 0.06 Gyr and 3.55 ± 0.06 Gyr. The figure also illustrates that the metallicity of the system components ranges from $Z = 0.03$ to $Z = 0.019$.

4.6. HIP 40523

The analysis for the HIP 40523 system was begun by assuming that it is a triple in *A*, mainly because the component *A* is confirmed as a sub-binary by Nordström et al. (2004) and Tokovinin (2019). The analysis for HIP 40523 as triple in *A* resulted in good fitting outcomes for both the main and sub-binary systems. This is proven based on the synthetic photometry results (see Table 2), as well as the comparison between the synthetic and observed photometry (see Table 3). Hence, HIP 40523 is a triple system that consists of the sub-binary *A* and the single star *B*, as explained by Tokovinin (2019). The adopted synthetic SED is shown in Figure 1(f). Referring to the adopted physical properties of HIP 40523 as a

Table 5
BMSSs That Have Been Analyzed by the Al-Wardat (2002) Technique between 2002 and 2021 That Were Used to Perform the *M–L* Relation Fitting

System	Components	Individual Mass ($M_\odot$)	Individual Luminosity ($L_\odot$)	Total Mass ($M_\odot$)	Total Luminosity ($L_\odot$)	Reference
HIP 59426	*A*a	0.99	1.27	3.50	2.80	This work
	*A*b	0.95	0.93	…	…	…
	*B*a	0.80	0.30	…	…	…
	*B*b	0.80	0.30	…	…	…
HIP 23824	*A*a	1.20	2.39	3.26	4.76	Yousef et al. (2022)
	*A*b	1.17	1.78	…	…	…
	B	0.90	0.59	…	…	…
HIP 101227	*A*a	0.90	0.45	3.42	1.52	Yousef et al. (2021)
	*A*b	0.90	0.45	…	…	…
	*B*a	0.81	0.31	…	…	…
	*B*b	0.81	0.31	…	…	…
HIP 9642	*A*a	1.05	2.0	3.25	3.62	This work
	*A*b	0.99	1.39	…	…	…
	*B*a	0.60	0.11	…	…	…
	*B*b	0.60	0.11	…	…	…
HIP 109951	*A*	1.10	1.05	2.58	1.35	This work
	*B*a	0.78	0.26	…	…	…
	*B*b	0.60	0.04	…	…	…
HIP 35733	*A*a	1.24	3.06	3.44	8.10	This work
	*A*b	1.24	2.59	…	…	…
	B	1.1	2.45	…	…	…
HIP 105947	*A*a	1.28	3.42	2.98	4.66	This work
	*A*b	0.88	0.25	…	…	…
	B	0.7	0.99	…	…	…
HIP 40523	*A*a	1.20	4.35	3.48	9.28	This work
	*A*b	1.20	4.35	…	…	…
	B	0.89	0.58	…	…	…
HIP 19206	*A*	1.23	2.84	2.14	3.68	Al-Wardat et al. (2021)
	B	0.91	0.84	…	…	…
HIP 84425	*A*	1.29	3.49	2.17	4.40	Al-Wardat et al. (2021)
	B	0.88	0.91	…	…	…
HIP 70973	*A*	1.01	0.39	1.91	0.65	Al-Tawalbeh et al. (2021)
	B	0.9	0.26	…	…	…
HIP 72479	*A*	0.94	0.61	1.79	1.02	Al-Tawalbeh et al. (2021)
	B	0.85	0.41	…	…	…
HIP 116259	*A*	1.18	1.63	1.93	1.88	Masda et al. (2019b)
	B	0.75	0.25	…	…	…
HIP 14075	*A*	0.99	0.71	1.95	1.30	Masda et al. (2018a)
	B	0.96	0.59	…	…	…
HIP 14230	*A*	1.18	1.94	2.02	2.42	Masda et al. (2018a)
	B	0.84	0.48	…	…	…
HIP 64838	*A*	1.75	12.38	3.07	19.63	Al-Wardat et al. (2017)
	B	1.55	7.25	…	…	…
Geilse 762.1	*A*	0.89	0.51	1.72	0.91	Masda et al. 2016
	B	0.83	0.40	…	…	…
COU 1511	*A*	1.17	2.09	2.23	3.17	Al-Wardat et al. (2016)
	B	1.06	1.08	…	…	…
HIP 25811	*A*	1.55	7.59	3.05	13.75	Al-Wardat et al. (2014c)
	B	1.50	6.16	…	…	…
HIP 689	*A*	1.35	4.63	2.60	8.27	Al-Wardat et al. (2014a)
	B	1.25	3.74	…	…	…
Geilse 150.2	*A*	0.83	0.56	1.43	0.66	Al-Wardat et al. (2014b)
	B	0.60	0.10	…	…	…
HIP 4809	*A*	1.6	15.84	3.06	31.67	Al-Wardat (2014)
	B	1.46	15.83	…	…	…
HIP 11352	*A*	0.99	0.82	1.94	1.52	Al-Wardat (2009)
	B	0.95	0.70	…	…	…
HIP 11253	*A*	0.93	0.70	1.82	1.32	Al-Wardat & Widyan (2009)
	B	0.89	0.62	…	…	…
COU 1289	*A*	1.55	5.13	2.81	7.9	Al-Wardat (2007)
	B	1.26	2.77	…	…	…
COU 1291	*A*	1.33	3.25	2.46	4.81	Al-Wardat (2007)

Table 5
(Continued)

System	Components	Individual Mass ($M_\odot$)	Individual Luminosity ($L_\odot$)	Total Mass ($M_\odot$)	Total Luminosity ($L_\odot$)	Reference
	B	1.13	1.56	...	...	...
ADS 11061	*A*a	1.24	5.74	4.96	15.37	Al-Wardat (2002)
	*A*b	1.17	3.85	...	...	...
	*B*a	1.32	3.20	...	...	...
	*B*b	1.23	2.58	...	...	...

triple system in *A* (Table 4), the positions of the system components on evolutionary tracks and isochrone tracks, and the age lines for both low- and intermediate-mass stars, are illustrated in Figure 2(f). This shows that the age of the system ranges between 3.55 and 3.98 Gyr, with a metallicity between 0.019 and 0.03. The positions of the components on the evolutionary tracks (see Figure 2(f)) gave the following individual masses: $M_{Aa} = 1.20 \pm 0.20 M_\odot$, $M_{Ab} = 1.20 \pm 0.20 M_\odot$, and $M_{Bb} = 0.89 \pm 0.20 M_\odot$.

5. Discussion

To summarize, our analysis has revealed that the systems HIP 109951, HIP 105947, HIP 35733, and HIP 40523 are more consistent as being triple systems, in agreement with past studies. However, in contradiction to previous studies, the systems HIP 9642 and HIP 59426 were found to be more consistent with being quadruple systems. In addition to these six systems, the remaining two systems in our sample, i.e., HIP 101227 and HIP 23824, were identified as quadruple and triple systems (Yousef et al. 2021; Yousef et al. 2022), respectively.

Based on the physical properties determined for the systems, we propose formation and evolution theories for them (Section 5.1), and discuss the applicability of the well-known *M–L* relations established by Eker et al. (2015) for the systems analyzed using the Al-Wardat (2002) method (Section 5.2).

5.1. Formation and Evolution of Binary and Multiple Systems

Based on our analysis, we have found that the stellar components within the same system have a similar age. This suggests that the fragmentation process is the most probable formation theory for all systems, as opposed to the capture theory, which usually results in different stellar ages within the same system. Hierarchical fragmentation during rotational collapse might produce binaries and multiple systems (Zinnecker & Mathieu 2001). This mechanism is possible if the spinning disk around an incipient central protostar is fragmented, as long as it continues to infall (Bonnell & Bate 1994).

5.2. Mass–Luminosity Relation

The Mass–Luminosity (*M–L*) relation was first established by Hertzsprung (1923) and Russell et al. (1923) independently, using the masses of visual binaries. Later, Eddington (1988) included eclipsing binaries in order to improve the relation. The *M–L* relation continued to be enhanced as the number of discovered binaries increased. To test the physical properties determined by the Al-Wardat (2002) method, we compare the *M–L* relation for all systems that have been analyzed by the technique from 2002 until 2021 (see Table 5) with the well-established relation by Eker et al. (2015) for the following mass ranges:

$$\left(\frac{L}{L_\odot}\right) = \begin{cases} \left(\frac{M}{M_\odot}\right)^{4.841}, & (0.38 M_\odot < M < 1.05 M_\odot) \\ \left(\frac{M}{M_\odot}\right)^{4.328}, & (1.05 M_\odot < M < 2.4 M_\odot) \\ \left(\frac{M}{M_\odot}\right)^{3.962}, & (2.4 M_\odot < M < 7.0 M_\odot). \end{cases} \quad (14)$$

Figure 3 (left) illustrates the *M–L* relation for the individual components of the systems. Overall, it can be seen that the physical parameters obtained by the Al-Wardat (2002) method agree very well with the *M–L* relation derived by Eker et al. (2015). The consistency is reflected in the positive values of Pearson's r and the coefficient of determination (R-square); i.e., 0.92 and 0.85, respectively. This demonstrates the reliability of the Al-Wardat (2002) method in determining the physical properties of the individual components of BMSSs.

Next, we also investigated the *M–L* relation for the entire binary, triple, and quadruple systems. We performed a linear fitting to our data and the results are shown in Figure 3 (right) and Equations (15), (16), and (17), for binary, triple, and quadruple systems, respectively. The statistics of the fitting are shown in Table 6. We were able to yield a good fit for the binary systems; i.e., Pearson's r and coefficient of determination values of ~1. For the triple and quadruple systems, decent fits were also obtained, however, due to the lack of data (the systems identified using the Al-Wardat (2002) method are limited), the relations may not be reliable. Nevertheless, based on Figure 3, we can deduce some general behaviors about the systems. For example, the relations for all binary, triple, and quadruple systems displayed similar slopes that are consistent within the uncertainties (Table 6).

$$\left(\frac{L}{L_\odot}\right) = \left(\frac{M}{M_\odot}\right)^{4.72}, (1.43 M_\odot < M < 3.07 M_\odot), \quad (15)$$

$$\left(\frac{L}{L_\odot}\right) = \left(\frac{M}{M_\odot}\right)^{5.07}, (2.58 M_\odot < M < 3.58 M_\odot), \quad (16)$$

$$\left(\frac{L}{L_\odot}\right) = \left(\frac{M}{M_\odot}\right)^{4.50}, (3.25 M_\odot < M < 4.96 M_\odot). \quad (17)$$

Our findings on the *M–L* relation for entire systems can potentially be used to estimate the nature of stellar systems in the future; i.e., either they are binaries or multiple systems. For instance, systems that are located under the binary line are more likely to be multiple stellar systems. Identifying more triple and quadruple systems will enhance the ability of the figure to determine if the system is a triple or quadruple stellar system.

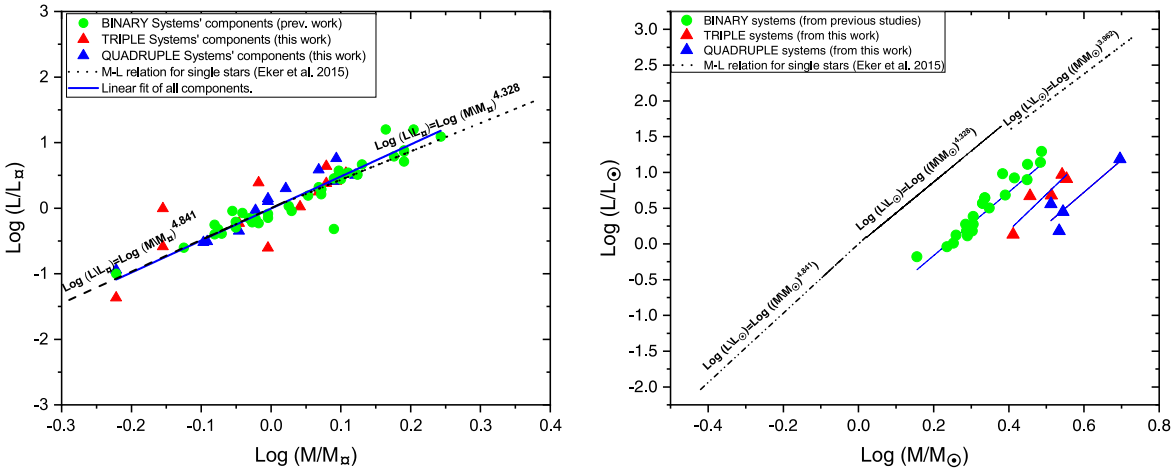

Figure 3. The Mass–Luminosity relation for the systems' individual components (left) and the entire systems (right), as studied by the Al-Wardat (2002) method between 2002 and 2021.

Table 6
The Fitting Statistics of *M–L* Relations for Different Orders of Stellar Multiplicities

Stellar Multiplicity	Slope	Pearson's r	R-square
Binary	4.72 ± 0.28	0.97	0.95
Triple	5.07 ± 1.2	0.92	0.84
Quadruple	4.50 ± 1.7	0.89	0.79

6. Conclusion

In this paper, we have presented an analysis of a sample of eight bright ($V \leqslant 10$ mag) and close ($d \leqslant 100$ pc) triple–stellar system candidates in our galaxy, to determine their true nature (i.e., triple or otherwise) and the physical parameters of each stellar component in the systems. The sample was studied using a spectrophotometric technique developed by Al-Wardat (2002) that utilizes model atmospheres from ATLAS9. According to our analysis, we found that five of the stellar systems (i.e., HIP 109951, HIP 105947, HIP 40523, HIP 35733, and HIP 23824) are indeed triple, while the remaining three systems (i.e., HIP 9642, HIP 59426, and HIP 101227) are more consistent with being quadruple. The physical properties of the individual stellar components were determined using the most recent parallax measurements obtained from the GAIA catalog. The similarity between the ages of the stellar components in each system suggests that the fragmentation process is the most probable formation theory for the systems.

In addition, we also tested the applicability of the well-established Mass–Luminosity (*M–L*) relation for individual components of all the stellar systems that have been analyzed by the Al-Wardat (2002) technique, including our sample. In general, we found that the parameters derived for the components using the method are consistent with the established relationship. This provides strong proof of the reliability of the Al-Wardat (2002) technique in determining the physical properties of BMSSs. We also investigated the *M–L* relation for each order of stellar multiplicity by performing linear fitting to the data we gathered. Based on this, we found that the slopes for each multiplicity are in agreement with each other within the uncertainties. The relations also seem to shift down in luminosity for a given total mass of the system, as the number of stellar components increases from binary to quadruple. Our results can potentially be applied in future studies to determine the multiplicity of stellar systems. However, due to the lack of data, particularly for higher-order systems, further study needs to be done in order to improve the relations.

We acknowledge financial support from Malaysia's Ministry of Higher Education Fundamental Research Grant Scheme code FRGS/1/2019/STG02/UKM/02/7. This work has made use of the Al-Wardat (2002) complex method for analyzing CVBMSs, which uses computer coding written in FORTRAN and the Interactive Data Language (IDL) of the ITT Visual Information Solutions Corporation.

This work has made use of data obtained from SAO/NASA, the SIMBAD database, the Fourth Catalog of Interferometric Measurements of Binary Stars, and the European Space Agency (ESA) mission GAIA (https://www.cosmos.esa.int/gaia), processed by the GAIA Data Processing and Analysis Consortium (DPAC, https://www.cosmos.esa.int/web/gaia/dpac/consortium). Funding for the DPAC has been provided by national institutions, in particular, the institutions participating in the GAIA Multilateral Agreement. All data are publicly available to access and download.

ORCID iDs

Z. T. Yousef https://orcid.org/0000-0002-6385-1385
A. Annuar https://orcid.org/0000-0003-0387-1429
Mashhoor A. Al-Wardat https://orcid.org/0000-0002-1422-211X
N. S. A. Hamid https://orcid.org/0000-0002-8674-5921

References

Aguilera-Gómez, C., Ramírez, I., & Chanamé, J. 2018, A&A, 614, A55
Al-Tawalbeh, Y. M., Hussein, A. M., Taani, A., et al. 2021, AstBu, 76, 71
Al-Wardat, M. 2002, Bull. Spec. Astrophys. Obs., 53, 51
Al-Wardat, M. 2007, AN, 328, 63
Al-Wardat, M. 2008, AstBu, 63, 361
Al-Wardat, M. 2009, AN, 330, 385
Al-Wardat, M. 2012, PASA, 29, 523
Al-Wardat, M. 2014, AstBu, 69, 454
Al-Wardat, M., Balega, Y., Leushin, V., et al. 2014a, AstBu, 69, 58
Al-Wardat, M., Balega, Y., Leushin, V., et al. 2014b, AstBu, 69, 198
Al-Wardat, M., Docobo, J., Abushattal, A., & Campo, P. 2017, AstBu, 72, 24
Al-Wardat, M., & Widyan, H. 2009, AstBu, 64, 365
Al-Wardat, M. A. 2002, BSAO, 53, 51
Al-Wardat, M. A., Abu-Alrob, E., Hussein, A. M., et al. 2021, RAA, 21, 161
Al-Wardat, M. A., El-Mahameed, M. H., Yusuf, N. A., Khasawneh, A. M., & Masda, S. G. 2016, RAA, 16, 166
Al-Wardat, M. A., Hussein, A. M., Al-Naimiy, H. M., & Barstow, M. A. 2021, PASA, 38, e002
Al-Wardat, M. A., Widyan, H. S., & Al-thyabat, A. 2014c, PASA, 31, e005
Apellániz, J. M. 2007, in ASP Conf. Ser. 364, The Future of Photometric, Spectrophotometric and Polarimetric Standardization (San Francisco, CA: ASP), 227
Balega, I., Balega, Y. Y., Maksimov, A., et al. 2006, Bull. Spec. Astrophys. Obs, 59, 20
Balega, Y. Y., & Tikhonov, N. 1977, SvAL, 3, 272
Bonnell, I. A., & Bate, M. R. 1994, MNRAS, 269, L45
Borkovits, T., Hajdu, T., Sztakovics, J., et al. 2016, MNRAS, 455, 4136
Borkovits, T., Rappaport, S., Kaye, T., et al. 2019, MNRAS, 483, 1934
Dommanget, J., & Nys, O. 2002, O&T, 54, 5
Duquennoy, A., & Mayor, M. 1992, Binaries as Tracers of Stellar Formation (Cambridge: Cambridge Univ. Press)
Ebert, R. 2001, The Formation of Binary Stars, Vol. 200, ed. H. Zinnecker & R. Mathieu, 573
Eddington, A. S. 1988, The Internal Constitution of the Stars (Cambridge: Cambridge Univ. Press)
Eker, Z., Soydugan, F., Soydugan, E., et al. 2015, AJ, 149, 131
Girardi, L., Bressan, A., Bertelli, G., & Chiosi, C. 2000, A&AS, 141, 371
Gray, D. F. 2005, The Observation and Analysis of Stellar Photospheres (Cambridge: Cambridge Univ. Press)
Halliday, D., Resnick, R., & Walker, J. 2013, Fundamentals of Physics (Hoboken, NJ: Wiley)
Hertzsprung, E. 1923, BAN, 2, 15
Hilditch, R. W. 2001, An Introduction to Close Binary Stars (Cambridge: Cambridge Univ. Press)
Horch, E. P., Falta, D., Anderson, L. M., et al. 2009, AJ, 139, 205
Koçak, D., İçli, T., & Yakut, K. 2020, CoSka, 50, 508
Labeyrie, A. 1970, A&A, 6, 85
Lang, K. 1992, Astrophysical Data: Planets and Stars (New York: Springer), 937
MacKnight, M., & Horch, E. 2004, BAAS, 36, 788
Mamajek, E., Torres, G., Prsa, A., et al. 2015, arXiv:1510.06262
Mardini, M. K., Frebel, A., Chiti, A., et al. 2022, ApJ, 936, 78
Masda, S., Docobo, J., Hussein, A., et al. 2019a, AstBu, 74, 464
Masda, S. G., Al-Wardat, M. A., Neuhäuser, R., & Al-Naimiy, H. M. 2016, RAA, 16, 012
Masda, S. G., Al-Wardat, M. A., & Pathan, J. 2018a, JApA, 39, 1
Masda, S. G., Al-Wardat, M. A., & Pathan, J. 2019b, RAA, 19, 105
Masda, S. G., Al-Wardat, M. A., & Pathan, J. K. M. K. 2018b, RAA, 18, 072
Masda, S. G., Al-Wardat, M. A., & Pathan, J. M. 2019c, RAA, 19, 105
Mason, B. D., Hartkopf, W. I., & Tokovinin, A. 2010, AJ, 140, 735
Monet, D. G. 1979, ApJ, 234, 275
Nordström, B., Mayor, M., Andersen, J., et al. 2004, A&A, 418, 989
Russell, H., Adams, W., & Joy, A. 1923, PASP, 35, 189
Stassun, K. G., & Torres, G. 2021, ApJL, 907, L33
Sürgit, D., Erdem, A., Engelbrecht, C. A., & Marang, F. 2020, MNRAS, 493, 2659
Tokovinin, A. 1992, in ASP Conf. Ser. 32, Complementary Approaches to Double and Multiple Star Research (San Francisco, CA: ASP), 573
Tokovinin, A. 2016, AJ, 152, 10
Tokovinin, A. 2019, AJ, 158, 222
Tokovinin, A. 2021, AJ, 161, 144
Van Leeuwen, F. 2007, A&A, 474, 653
Yousef, Z. T., Annuar, A., Al-Wardat, M., & Hamid, N. S. A. 2022, Malaysian J. Sci., 43, 10001
Yousef, Z. T., Annuar, A., Hussein, A. M., et al. 2021, RAA, 21, 114
Zinnecker, H., & Mathieu, R. D. 2001, in IAU Symp. 200, The Formation of Binary Stars (San Francisco, CA: ASP)